Diamond and cBN hybrid and nanomodified cutting tools with enhanced performance: Development, testing and modelling

Loginov, Pavel; Mishnaevsky, Leon; Levashov, Evgeny; Petrzhik, Mikhail

Published in:
Materials & Design

Link to article, DOI:
10.1016/j.matdes.2015.08.126

Publication date:
2015

Document Version
Peer reviewed version

DIAMOND AND CBN HYBRID AND NANOMODIFIED CUTTING TOOLS WITH ENHANCED PERFORMANCE: Development, testing and modelling

Pavel Loginov[1], Leon Mishnaevsky Jr.[2*], Evgeny Levashov[1], Mikhail Petrzhik[1]

[1]National University of Science and Technology "MISIS", Moscow 119049, Russia,
[2] Department of Wind Energy, Technical University of Denmark, Roskilde, Denmark

Abstract:
The potential of the enhancement of superhard cutting tool performance on the basis of microstructural modifications of the tool materials is studied. Hybrid machining tools with mixed diamond and cBN grains, and machining tools with composite nanomodified metallic binders are developed, and tested experimentally and numerically. It is demonstrated that both combinations of diamond and cBN (hybrid structure) and nanomodification of the metallic binder (with hexagonal boron nitride/hBN platelets) lead to sufficient improvement in the machining performance. Superhard tools with 25% of the diamond replaced by cBN grains demonstrate 20% increased performance as compared with pure diamond machining tools, and more than two times higher performance compared with pure cBN tools. Furthermore, the machining efficiency of the wheels modified by hBN particles was 80 % more efficient compared with the tools with the original binder. A computational model of hybrid superhard tools is developed, and applied to the analysis of the structure-performance relationships of the tools.

Keywords: Composites; Nanoreinforcement; Machining tool

1. Introduction

The productivity of cutting tools from superhard materials (SHM) determines the quality and costs of manufacturing many industrial products. The performance of machining tools depends to a large degree on the microstructural parameters of the tools, e.g., binder properties, cutting grain distribution and strength, and grain/binder bonding [1-6].

The problem of the enhancement of material properties by tailoring material structures is one of the most important challenges of materials science [7]. The potential of nanoengineering technologies, nanostructuring and nanomodification has been studied intensively over the last decades, and also been proven to open new possibilities in the material improvement [8-13].

* Corresponding author, Email: lemi@dtu.dk. Phone: 45 4677 5729. Fax: 45 4677 5758

Another approach, which has attracted growing interest recently, is hybridization, i.e., the combination of different constituents in a single material that should support and complement one another [9]. Considering machining tools as superhard particle reinforced composites, one can transfer some of the techniques of the improvement of other groups of composites to improve the machining tool efficiency. Several authors used nanomodifications to improve grinding wheel performance [**13**-**18**]. Suzuki and Konno [**18**] used Ni-CNT composite coatings to improve the grain bonding strength in electroplated diamond tools. They demonstrated an eight times better lifetime of tools with Ni-CNT coatings than those without them. Jung et al. [**19**] added CNTs into magnetorheological fluids for a magnetorheological finishing process. Sidorenko, Levashov et al. [20, 21] developed metallic CNT (carbon nanotube)-reinforced binders for diamond drilling wheels, achieving drastically improved wheel performances. Jakob and colleagues [22] developed new sintered metal matrix (Co, modified by Fe or Ni) composite cutting materials for heavily reinforced concrete structures. In so doing, the authors also considered hybrid reinforcements (WC + diamond, diamond+, cBN) embedded in a cobalt-based binder. The authors have proven that the cBN+diamond reinforced grinding wheels show the best ratio of the amount of removed concrete to wear.

Still, the microstructural improvement of machining tools, including nanostructuring and hybridization, is a relatively new subject.

In this paper, we seek to explore the potential effects of hybrid and nanomodified structures of cutting tools using superhard materials on their service properties. Hybrid drilling tools with varying portions of diamond and cBN grains were investigated in experiments and computational studies. The wear and productivity of such hybrid cutting tools were determined for different fractions of diamond and cBN. To explore the effect of nanoreinforcements, Fe/Cu/Co based metallic binders with and without hexagonal boron nitride (hBN) nanoparticle reinforcement have been manufactured and tested. A computational model of machining by a superhard hybrid tool and the resulting tool wear is developed.

2. Hybrid diamond/cBN cutting tools: Optimization of composition and structures

Diamond monocrystals are typical abrasive elements of segmental cut-off wheels for concrete cutting. Their advantages over other SHMs include their high hardness as well as static and dynamic strength. Because cutting using cut-off wheel tools is performed at 1500–3000 revolutions per minute (rpm), the ability of SHM grains to stay intact under constant

mechanical loads is essential. The resistance of SHMs to chemical wear is also critical for cutting steel or cast iron. This wear results from diamond graphitization followed by carbon diffusion to the material being treated. To develop high quality cutting tools for steels and cast irons, two problems need to be addressed: 1 – to increase the hardness, strength and impact resistance of a binder and ensure its ability to securely retain the SHM grain [**23**-**25**]; 2 – to ensure the undamaged condition and integrity of SHM grains for the low wear of the binder.

While using diamond to manufacture rope saws and segmental cut-off wheels for cutting steel and cast iron is undesirable due to the chemical wear caused by diamond graphitization, synthetic diamond powders are still rather widely used as SHMs [**26**,**27**]. The effect of the chemical wear of SHM on the performance of a tool can be reduced by partial replacement of the diamond in the tool's working layer with cBN, which is chemically inert to Fe [**28**]. However, the strength of cBN monocrystals is four times lower than that of diamonds, so they are more likely to be mechanically destroyed. Hence, it is vital to find the optimal diamond-to-cBN ratio in the binder for cutting tools for steels and cast irons.

In this section, hybrid machining tools from superhard materials (diamond and cBN) are manufactured and tested, to clarify the wear mechanisms in such tools.

2.1 Composition and structures of binder and hybrid diamond / cBN tools

Manufacturing. Composition 35% Cu – 17% Fe – 18% Co – 30% Ni (hereinafter referred to as N) was taken as the original binder to manufacture cutting tools for steels and cast irons. The primary components to prepare this binder were Next100 Cu-Fe-Co alloy powder (Eurotungstene, France) and PNK-UT3 carbonyl nickel powder (OAO Kola Mining and Metallurgical Company, Russia.) Components were mixed in a ball mill for 3 h. The resulting mixtures were used to produce compacted samples 55×10×3 mm in size with a residual porosity of 3.5 % by hot pressing. Hot pressing was performed using a Dr. Fritsch DSP-475 setup in an inert atmosphere at 850 ºC, 350 MPa (isobaric exposure for 3 min).

Mixtures of binder N components with super-hard material (SHM) powders were prepared to manufacture beads and segments of cutting tools (diamond and cBN) prior to hot pressing. We used a SDB1100 monocrystalline diamond powder (Element Six) with a characteristic cuboctahedron shape of the grain and cubic boron nitride powder (cBN, ABN 605 grade). cBN powder consists of equiaxial chipped grains (Fig. 2). The static strength of these types of SHM was determined experimentally according to the State Standard (GOST) 9206-80 (two samples, 50 grains each.) The average strength of a diamond grain is 320 N, and 80 N for cBN. Thus, the static strength of diamond is four times as high as that of cBN.

Occasional metal inclusions distributed in the grains of SDB1100 diamond crystals ensure high thermal resistance, up to 1100 °C. Meanwhile, the ABN605 powder is characterized by high strength compared to other cBNs.

The relative concentration of SHM in the binder was determined based on the content of 20 vol. % in the working layer. Figure 3 shows the failure pattern of a diamond-containing segment with binder N. In addition to the diamond grains tightly connected to the binder, there are also traces of pulled out diamond grains.

Structure of metallic binder and tool. Vigorous copper diffusion into the nickel grains during hot pressing results in the formation of two phases: Ni-Cu and Fe-Co solid solutions (Table 1.)

The structure of the hot-pressed binder N consists of rounded and oblong light Cu-Ni grains enclosed in a dark matrix of Fe-Co solid solution (Fig. 1.) EDX studies showed that the grains of the Cu-Ni solid solution are nickel-rich in the centre and copper-rich at the periphery. The concentration gradient of copper with respect to the Cu-Ni solid solution grain confirms that this phase is formed via a diffusion mechanism. Isobaric exposure during hot pressing for more than 3 min makes the concentration gradient decrease to total disappearance due to grain homogenization.

2.2 Effect of hybrid diamond/cBN structures on the wear mechanism and cutting rate

Experiments: To determine the optimal diamond-to-cBN ratio in the tool's working layer, a pilot batch of beads was manufactured. The beads were fully manufactured at Dr. Fritsch process line (Germany). The beads were tested for steel cutting at the experimental facility. This facility basically consists of two electric motors. The first one is fixed to the frame. The rotating speed of its output shaft is 250 rpm. The workpiece, a disk made of Steel 3, is attached to the output shaft. The second electric motor is fixed to the moving frame. The rotating speed of its output shaft is 60 rpm. A pin with a bead fastened to it is attached to that motor by a threaded connection. Before starting the test, the second motor is fixed with a spring, and the pin with the bead is pressed against the disk. This facility is equipped with a water cooling system. The maximum flow rate is 1 l/min. Each bead was tested for 90 min.

SHM grains were added to binder N in the following ratios (in weight %): 100% diamond; 75% diamond + 25% cBN; 50% diamond + 50% cBN; and 25% diamond + 75% cBN.

Figure 4 shows the test results. The workpiece was shaped like a disk and cut on the lateral side. It was impossible to determine the exact area of the cut, as it did not run through the entire disc thickness. Therefore, the performance was defined by the loss in disk weight (g). The beads with 25% of the diamond replaced with cBN grains demonstrated the maximum

performance until the cutting properties were completely lost. The performance improved by 20% in this case. The performance significantly deteriorated as the cBN content was further increased.

Mechanisms of cutting and wear in superhard cutting tools. In cutting steels and cast irons, plough abrasive chips are produced that barely open the working layer. Diamond grains almost never fail upon contact with a workpiece. However, the cutting process is associated with high temperatures, and metal catalysts (Fe and Ni) cause chemical erosion (wear) of diamonds (Fig. 5.) Cutting edges and diamond crystal facets gradually become rounded and smooth, thus reducing diamond retention in the binder and the cutting rate of the tool [1]. The cutting mechanism of the cBN grains is different, as their faceting is irregular and they do not react with steel and cast iron. The wear of cBN grains is not associated with the smoothening of facets. The relatively low strengths of the cBN grains result in numerous micro-cleavages, and new sharp facets and edges are formed. The irregular shape securely keeps cBN in the binder. Therefore, the cBN content in the working layer remains virtually constant during the entire treatment time. The fast mechanical destruction of cBN is the only reason why the diamond cannot be fully replaced by cBN. The low wear of the binder and the impossibility to open new SHM layers result in the glazing of the working layer. This halts the cutting process and requires the opening of the SHM using special equipment.

The experimental results confirm that the cutting and wear mechanisms for diamond- and cBN-containing cutting tools are different. The performance depends on the cBN content, as cutting involves two competing processes. On the one hand, diamond graphitization at the interface with the binder, chemical wear and the smoothening of facets, as well as the pulling out of the working layer, can be observed. On the other hand, cBN grains are securely retained are faster worn mechanically. To prove this hypothesis, the SHM condition in the beads after testing was assessed. The bead surface was examined using optical microscopy. All of the detected SHM grains (or pits left after their pullout) were divided into three groups: intact, blunted and pulled-out (see columns "Intact", "Blunted" and "Pulled-out" in Fig. 4.)

As shown in the diagram (Fig. 4), the reduced diamond content in the working layer results in fewer SHM grains being pulled out from it. This is caused by a more secure retention of cBN due to its irregular shape. Figure 6 shows an image of a bead with a 75/25 diamond to cBN ratio after testing. As we can see, the cBN grains stay in the working layer, while there are pits instead of diamond grains. The shape of the pits is also cuboctahedral.

3. Hierarchical nanoreinforced diamond/cBN cutting wheels: Structure and composition

With a view on using the potential of nanomodification to improve the efficiency of cutting tools, a number of various nanoparticles have been explored as potential additions to the metallic binder of cutting tools, including WC, ZrO_2, Al_2O_3, CNT, hBN, see [20, 21, 29]. However, the most promising preliminary results for this tool/material system were obtained when hBN was added. Unlike other nanoreinforcements, hexagonal boron nitride is chemically inert with respect to both iron and diamond, and acts as a dry lubricant at elevated temperatures. Therefore, along with the effect of the dispersion hardening of the metal binder (see below), it is expected to form a thin layer on diamond grains, reducing direct contact with metal diamond - catalysts (Fe, Co, Ni), and protecting the diamond surface from graphitization both under hot pressing and during the cutting of cast iron.

3.1 hBN reinforcement: Powder mixture preparation and sample manufacturing

Hexagonal boron nitride (hBN) powder was used to modify binder N. The modifying agent has a low concentration and a significantly different density compared to powders of the original binder N, which is a problem. Therefore, the mixture was prepared in a planetary ball mill (PBM) in air at a centripetal acceleration of 28 g. This treatment method helped avoid segregation and ensured the even distribution of the modifying agent. Furthermore, hBN is repeatedly refined during the mixing (Fig. 7.) The initial hBN powder used in this study is an assembly of particles with lamellar and rounded structures (Fig. 7a). They are approximately 1 μm thick and are 5 μm or more in diameter. After the mixture is treated in the PBM together with the binder N components for 3 min, no particles larger than 200 nm are left in it (Fig. 7b.) The original binder components are evenly distributed.

The XRD data show that only phases present in the initial α-Fe and Cu (components of Next100) and Ni powders are observed in the mixture (Table 2).

Compacted samples 55×10×3 mm in size were produced by hot pressing, and their mechanical properties were defined to determine the optimal concentration of hBN nanomodifier. hBN content, between 0.01 and 1 wt %. The mechanical properties of the original binder (without nanomodifier) were tested for reference. The original binder was prepared in a ball mill (N) and in a PBM (N “0”).

3.2 *Structure of metallic binder with and without hBN reinforcement*

The structure of the metallic binders was investigated by means of optical and electron microscopy and X-ray diffraction analysis.

According to the data in Table 1, hot pressed binder N contained two phases – Cu-Ni-based and Fe-Co-based solid solutions - in a mass ratio of 70 : 30. The same result was obtained for the binder with hBN reinforcement.

The average grain size of the Cu-Ni phase (light grey areas in Fig. 8 a, b) computed using Imagescope software in the original and modified binder was 4.70 and 3.85 μm, respectively. The average grain size of the Fe-Co phase was determined at fractures by the chord length measuring technique, with more than 1000 measurements for each type of grain, as prescribed by the State Standard (GOST) 5639-82. Following the addition of hBN, the average grain size of the Fe-Co phase decreases by nearly 50%, from 0.95 to 0.64 μm. Thus, hBN influences the structure and properties of binder N by preventing recrystallization during the hot pressing. hBN particles that do not react with any component of binder N slow down the migration of grain boundaries and agglomerates.

The aspect ratios of the Cu-Ni grains were calculated using Imagescope software. The value of the aspect ratio for binder N was – 1,116 and for binder modified with hBN was – 1,203.

It was observed by means of scanning electronic microscopy and EDX that hBN platelets tend to be located at the grain boundaries of the Fe-Co phase after hot pressing (Fig. 7 b). This tendency occurs due to the larger surface area of Next100 particles, upon which the Fe-Co phase is based. Therefore, it is more likely that hBN platelets cover the Fe-Co grains. Additionally, hBN, an inert modifying agent, acts as a diffusion barrier between the Cu and Ni particles at hot pressing. This prevents the interdiffusion of Cu and Ni atoms and thereby the formation of the Cu-Ni phase.

As seen (Fig 7b), hBN platelets are mostly arranged parallel to each other, with a small deviation of +/-10 degrees.

3.3 *Metallic binder with hBN reinforcement. Mechanical properties*

In the experiments, the mechanical properties of hBN reinforced binder and the effects of intense mechanical treatment on the porosity, hardness and ultimate bending strength were evaluated.

Table 3 shows that the pretreatment of a powder mixture in the PBM has a negligible impact on the mechanical properties of a binder. The addition of hBN results in a significant simultaneous improvement of hardness and strength. The maximum effect is achieved when the hBN content is 0.1 wt %. The hardness increases by 7 HRB, and the strength by 160–180 MPa. With a

higher hBN concentration, a considerable part of the binder powder surface is suppressed and sintering is hindered, thus resulting in increased porosity and deterioration of properties.

The hardness (H, GPa) and elasticity modulus (E, GPa) were measured using the matrix nanoindentation method on polished hot-pressed parallel-sided samples, N and N – 0.1 % hBN. These measurements were made using a Nano-Hardness tester, a high-precision nanohardness tester (CSM Instruments), according to the Oliver–Pharr method [**31**]. A diamond triangular pyramid was used as an indenter (Berkovich indenter). The indentation load was 8 mN, the loading rate was 0.36 mN/s, and the exposure time at a peak load was 5 s. Indentation was carried out with a 20 μm increment towards the X axis and 15 μm towards the Y axis. These increments ensure that the indentations were made on different structural components. The matrix contained a total of 100 indentations [**32**].

The area containing the indentations was studied by optical microscopy. According to the observations, the binders under study had 3 structural components, corresponding to the Cu-Ni and Fe-Co phases and pores. All of the determined H and E values were then divided into two groups depending on the area they were in. When the indenter hit a pore, a dip appeared in the indentation curve. In this instance, H and E values were ignored.

The results of indentation tests (Table 4) demonstrate that the H and E values of both structural components of the N "0" binder are lower than those of N-0.1 % hBN (hardness by 10–20 %; elasticity modulus, by 5–10 %).

Figure 9 shows the typical load curves for the Cu-Ni (a) and Fe-Co (b) phases of N "0" and N-0.1 % hBN samples. The curves were built based on the results of the indentation tests. When testing the N "0" binder, the imprints were deeper for both phases. This implies that their hardness values are lower than those in the samples with hBN.

The tensile strength was measured on a Zwick Z250 universal testing machine (Germany) equipped with a sensor for determining the relative elongation to describe the volumetric strength parameters of the modified binders. The samples were subjected to tension at a rate of 4 mm/min. Three test samples of each composition were manufactured by hot pressing followed by electroerosion cutting. The samples were 55 mm long and had 4 × 2.5 mm rectangular cross-sections. The average bending strength of binder N modified by hBN particles is higher by more than 100 MPa (Table 5.)

4. Computational modelling of diamond and cBN based machining tools

4.1. Modelling machining tools as composites

Superhard grain based machining tools represent two-phase composites consisting of diamond or cBN grains and metallic or other binder. That makes it possible to apply material design approaches and methods of microstructural enhancement of material performance (see, e.g., [7]) to the improvement of the machining tool performances. A peculiarity of the machining tools, which are loaded on the surface (and not so much in volume as other structural composites) is the two-dimensional (surface) microstructure evolution under loading. In this point, the damage evolution in machining tools has some similarity with that in unidirectional composites, where the main local performance losses (like fibre failure or kinking) also have a two-dimensional effect due to the superhard grain failure.

4.2. Computational model of the wear and efficiency of superhard machining tools

To analyse the wear and evolution of the efficiency of superhard machining tools, a computer program has been developed. The computational code is based on the version presented in [32] and used for hybrid and hierarchical composites. The code interactively generates unit cells with a pre-defined number of superhard grains randomly arranged using the RSA (random sequential absorption) algorithm. The grains are assigned properties of cBN or diamond using the Monte-Carlo method. The code was written on Compaq Visual Fortran/Simply Fortran.

The machining process is simulated as follows. We consider the cut-out of the tool working surface, including N=100 grains. The runs of the tools correspond to the loading cycles in [9]. After each run, the diamond grains are worn out to some degree, creating a plane surface on each of them, and the load on each of them increases. At the same time, each cBN grain can be cracked or torn out of the binder. Further, the binder is worn out (by debris, water, etc.), increasing the heights of the grains. The heights of the grains are supposed to be random numbers following a Gaussian distribution and are calculated as follows:

$$h = h_0 + \Delta h_1 - \Delta h_2 - h_3; \qquad (1)$$

where h – current height of a given grain, h_0 - initial height, given as random value distributed by Gaussian law, Δh_1 - increase of the grain height as a result of the wearing out of the binder, Δh_2 - reduction of a grain height due to the blunting of the grain tip (only for diamonds), h_3 - reduction of the height due to random events of grain failure (cBN) or grain pull out. The chip thickness a is calculated as a= h - Δ, where Δ – a is the distance from the binder surface to the sample surface. The force on a grain is given as:

$$F = F_{av}(h - \Delta)^2 / a_{av}; \qquad (2)$$

where F and a – force and chip thickness for a given grain, *av* – index for average values over all grains.

The rate of binder wear and the likelihood of the cBN grain detachment are apparently interrelated and linked to the binder strength (stronger binder leads to slower wear and better interfacial strength between cBN and the binder) [1,4,5]. Here, we assume them to be proportional.

$$\sigma_{dia} = k_1 S\ ;\ \Delta h_3 = k_2 - k_3 S; \qquad (3)$$

where S – strength of binder, Δ – linear wear of binder after each run, σ_{dia} – tearing out stress of a diamond grain, $k_{1,2,3}$ – coefficients. The rate of material removal Q and the wear W per run are calculated as:

$$Q = \sum_N la^2\ ;\ W = \sum_N \mathrm{Pr}_{Failure} * v; \qquad (4)$$

where a – chip thickness, l – length of cut, $\mathrm{Pr}_{Failure}$ – probability of failure for each grain, v – volume of removed or failed grains.

The strengths of superhard grains are taken as follows: diamond 320 N, cBN – 80 N. Volume content of grains was 20%. The grain sizes are 350-400 μm (both diamond and cBN) and taken as 375 in the simulations. To estimate the load on the grains, a 3D finite element model of the cutting tool has been produced and run. Figure 11 shows the model and the stress distribution in the grains. It can be seen that the stresses are apparently localized in the small contacting area of the grains.

Figure 12 shows the schema of the simulation code and examples of the generated unit cells (20% and 34% of grains on the surface) (the unit cell models are visualized by the code as postscript-files). Figure 12d shows the unit cell with some failed diamond (black filling) and cBN grains (green filling). One can see that grains tend to fail close to already failed grains. Figure 13 shows some results of simulations: fraction of failed grains versus run curves.

4.3. Effect of binder structure and hBN reinforcement on the mechanical properties of the matrix

To estimate the influence of the binder structure on the performance, a micromechanical analysis of the mechanical properties of the binder with and without nanoreinforcement has been carried out. hBN platelets were taken as discs 18 nm (thickness) x 72 nm (radius). The Young modulus of the hBN platelets is taken as 675 GPa (see panadyne.com). To evaluate the effect of the nanoreinforcement on the mechanical properties, the micromechanical model of Halpin-Tsai [34] modified by Lewis and Nielsen [35] was used. The elastic properties of the nanoreinforced FeCo phase are calculated using the Halpin-Tsai equation for aligned platelets:

$$E = E_{FeCo}\left(\frac{1+\zeta\eta v_{hBN}}{1-\eta v_{hBN}}\right);\ \eta = (E_{hBN}/E_{FeCoi}-1)/(E_{hBN}/E_{FeCoi}+\zeta); \qquad (5)$$

where E- Young modulus, ζ and η - fitting coefficients, v_{CuNi} - volume content of hBN phase, 70%. The estimated value of the Young moduli for the Fe-Co matrix with hBN reinforced material is 181,4 GPa. This value is sufficiently lower than the value of the Young modulus for the Fe-Co-hBN matrix presented in Table 4 (194 MPa). Practically, it means that the higher mechanical properties of the nanomodified binder are controlled not only by the mechanical reinforcement effects but also by the reduced grain size of the material during the manufacturing with nanoadditives.

To evaluate the effect of the nanoreinforcement on the performance of the machining tool, the correction coefficient is introduced. The value S in the formula (1) is multiplied by a coefficient, obtained as a ratio of the strength of matrix in Table 5 (1.214=680/560 MPa). Figure 13b shows the fraction of teared diamond grains and of the total grains in softer and stiffer binders. One can see that the difference is quite visible, especially after a high number of runs.

To compare the numerical model and the experiments, we determined the fraction of pulled out grains (only diamonds) for different fractions of cBN grains in the tool. The experimental data (from Figure 4) and simulated results are shown in Figure 13c. It can be seem that the simulated results are quite close to the experimental data.

Comparing Figures 4 and 13, one can explain the peak at the 25% cBN/75% diamond tool in Figure 4. Apparently, the cBN destruction starts earlier than the chemical dulling begins to influence the sharpness of diamond grains, and they begin to pull-out. Thus, the fraction of failed cBN grains is higher at the beginning (Figure 13a). Then, the diamond grain peaks are chemically and thermally dulled and worn out, which increases the stress and load on the grains (also reducing the chip thickness and rate of material removal). After some time, the rate of the diamond grain pull-out increases drastically. Still, even after many diamond grains are pulled out or are dulled, the damaged (but still working) cBN grains continue to remove the work material. This ensures the potential for the increased efficiency of the hybrid cBN+diamond toolscompared with pure diamond tools.

5. Cutting cast iron by hybrid and hBN nanoreinforced diamond/cBN tools

Segmental cut-off wheels with N and N – 0.1 % hBN binders were tested using an Almaz-3 bridge cutting machine (Russia.) The machine was water cooled. The maximum flow rate

during testing was 10 l/min. The rotation speed of the segmental cut-off wheels was 3000 rpm. The diamond to cBN ratio in the working layer was 75/25. The diameter of the segmental cut-off wheels was 500 mm, and the segment size was 40 × 4.2 × 9 mm. The tools were tested until the cutting efficiency was totally lost and the working layer had to be reopened.

Figure 14 demonstrates that the segmental cut-off wheel with the N binder modified by hBN particles was 80 % more efficient compared to the tool with the original binder. The first reason is the effect caused by binder strengthening. As a result, its resistance to cutting loads and the diamond retention properties are enhanced. An analysis of the segment surface after the test showed that diamond grains pulled out of the binder were virtually absent. With hBN added, the binder at SHM grain boundary is worn to a lesser extent. Adhesion of the binder to the material being treated in the contact zone at high temperatures is prevented. Moreover, hBN partially covers the surface of the diamond grains and prevents their contact with metal catalysts (Fe, Co, Ni) and, consequently, graphitization during hot pressing.

Given the improvement in the tool performance achieved by the separate hybrid structure (20%) and nanomodified binder (up to 80%), the idea appears to combine these two effects. Works on the optimization of machining tool with hybrid superhard grains and a nanoreinforced binder are under way now. The expected increase in the machining tool productivity is far over 100%. As one of the results, a patent application for a new advanced cutting tool for machining steels and cast iron has been prepared and filed [36]. The patent application is under consideration now.

6. Conclusions

In this paper, the potential of microstructural modifications of superhard machining tools for the enhancement of their performance is studied. Hybrid machining tools with mixed diamond and cBN grains, as well as machining tools with composite nanomodified metallic binder, are developed and tested experimentally and numerically.

It is demonstrated that the suggested structural modifications of the machining tools ensure the improvement of machining performances in both cases. The superhard tools with 25% of diamond replaced by cBN grains demonstrate 20% increased performance compared with pure diamond machining tools and more than two times higher performances compared with pure cBN tools. Furthermore, the machining efficiency of the wheels modified by hBN particles was 80 % more efficient compared to the tools with the original binder.

Acknowledgements: The authors gratefully acknowledge the financial support of the Ministry of Education and Science of the Russian Federation in the framework of the “Program to

Increase the Competitiveness of the NUST “MISIS” among Leading Global Scientific Educational Centers” in 2013–2020 (project no. K2-2014-012).

References:

1. L. Mischnaewski. Wear of Grinding Wheels. Naukova Dumka, Kiev, 1982
2. B. Anand Ronald, L. Vijayaraghavan, R. Krishnamurthy. Studies on the influence of grinding wheel bond material on the grindability of metal matrix composites. Materials and Design 30 (2009) 679–686
3. J. N. Boland and X.S. Li, Microstructural Characterisation and Wear Behaviour of Diamond Composite Materials Materials 2010, 3, 1390-1419; doi:10.3390/ma3021390
4. L. Mischnaewski. (1985). Optimization of parameters of superhard drilling tools in griunding metals. J. Superhard Materials, 7(3) 45-49
5. L. Mischnaewski.: Verschleiss von Diamant- und CBN-Scheiben beim Schleifen zäher Metalle. Ind.Diam.Rdsch. , 1993, t. 27, nr 1, s. 50-54.
6. Bianchi, EC, Aguiar, PR, Monici, RD, Daré Neto, L, & Silva, LR da. (2003). Analysis of the performance of superabrasive and alumina grinding wheels with different bonds and machining conditions. Materials Research, 6(2), 239-246
7. L. Mishnaevsky Jr, Computational Mesomechanics of Composites, John Wiley, 2007, 280 pp.
8. G.M. Dai, L. Mishnaevsky Jr , Carbone nanotube reinforced hybrid composites: computational modelling of environmental fatigue and usability for wind blades, Composites Part B (2015), pp. 349-360.
9. L. Mishnaevsky Jr., G.Dai, Hybrid and hierarchical nanoreinforced polymer composites: Computational modelling of structure-properties relationships, Composite Structures, 117 (2014) 156–168
10. Bakshi, S.R.; Lahiri, D.; Agarwal, A. Carbon nanotube reinforced metal composites-a review. Int. Mater. Rev. 2010, 55, 42–64
11. SC Tjong, Carbon Nanotube Reinforced Composites: Metal and Ceramic Matrices, Wilet, 242 pp, 2009
12. N. Silvestre, State-of-the-art Review on Carbon Nanotube Reinforced Metal Matrix Composites, International Journal of Composite Materials2013; 3(6A): 28-44
13. J. You, Y. Gao A Study of Carbon Nanotubes as Cutting Grains for Nano Machining, 2009, Advanced Materials Research, 76-78, 502
14. You, J.L. Carbon nanotube grinding wheel for nano machining of engineering and biomedical materials 2009, MSc Thesis , Hong Kong University of Science and Technology
15. T. Suzuki, T. Mitsui, T. Fujino, M. Kato, Y. Satake, H. Saito and S. Kobayashi, Development of CNT-Coated Diamond Grains Using Self-Assembly Techniques for Improving Electroplated Diamond Tools Key Engineering Materials, Vol. 389-390(2009), p. 72-76
16. T. Suzuki, M. Kato, H.Saito, H,i Iizuka Improved Adherence Strength between Diamond Grains and Electrolytic Nickel Bonds by Carbon Nanotube Coatings, J Solid Mechanics and Materials Engineering , vol. 5, pp.386-396, 2011
17. T, Suzuki, M, Kato, H, Saito, H,Iizuka, Effect of Carbon Nanotube (CNT) Size on Wear Properties of Cu-Based CNT Composite Electrodes in Electrical Discharge Machining, J Solid Mechanics and Materials Engineering , vol. 5, pp.348-359, 2011
18. T. Suzuki T. Konno, Improvement in tool life of electroplated diamond tools by Ni-based carbon nanotube composite coatings Precision Engineering, 2014, 38, 3, 659-665
19. B. Jung, , K. Jang, B. Min, S.J. Lee and J. Seok: International Journal of Machine Tools and Manufacture, Vol. 49(2009), p. 407-418
20. Sidorenko D. A., Zaitsev A. A., Kurbatkina V. V., Levashov E. A., Andreev V. A., Rupasov S. I., Sevast’yanov P. I. Influence of additives of carbon nanotubes on the structure and properties of metal binders for a diamond tool // Russian Journal of Non-Ferrous Metals. 2013. Vol. 54, No. 6, P. 527 –531
21. D. Sidorenko, L. Mishnaevsky Jr, E. Levashov, P. Loginov and M. Petrzhik, Carbon nanotube reinforced metal binders for diamond cutting tools: Effect of CNT reinforcement on structure, properties and performances Materials and Design, doi: 10.1016/j.matdes.2015.06.056
22. Jakob, H.; Hassel, Th.; Köhler, A.; Bach, Fr.-W. (2011): MMC based materials as an alternative cutting material for cutting densely filled and heavily reinforced concrete structures, Proceedings of 1st International Conference on Stone and Concrete Machining. 1st International Conference on Stone and Concrete Machining. Hannover, 23.11.2011.

23. P. M. Amaral, A. Coelho, C. A. Anjinho, et al. Evaluation of the Relationship between Diamond Tool Wear Performance and the Mechanical Properties of the Individual Metallic Binders // Advanced Materials Forum V. 2010. – Vol. 636-637. – P. 1467-1474.
24. V A Konovalov, V A Aleksandrov, M D Levin. Influence of the strength of diamond containment and the rate of abrasive wear of a binder on the serviceability of a diamond-abrasive stone-cutting tool. – Sintech. Almaz. 1975. – p. 26-28.
25. G.P. Bogatyreva, G.F. Nevstruev, G.D. Il'nitskaya, V.A. Konovalov, V.N. Tkach. The possibilities for improvement of the strength of diamond grit retention in a binder // Sverkhtverdye Materialy. 2001. – Iss. 2. – P. 20-25.
26. B.M. Lane, M. Shi, T.A. Dow, R. Scattergood. Diamond tool wear when machining Al6061 and 1215 steel // Wear. 2010. – Vol. 268. – Iss. 11-12. – P. 1434-1441.
27. Y. Song, K. Nezu, C.-H. Park, T. Moriwaki. Tool wear control in single-crystal diamond cutting of steel by using the ultra-intermittent cutting method // International Journal of Machine Tools and Manufacture. 2009. – Vol. 49. – Iss. 3-4. – P. 339-343.
28. K.S. Neo, M. Rahman, X.P. Li, H.H. Khoo, M. Sawa, Y. Maeda. Performance evaluation of pure CBN tools for machining of steel // Journal of Materials Processing Technology. 2003. – Vol. 140. – Iss. 1-3. – P. 326-331.
29. P.A. Loginov, E.A. Levashov, V.V. Kurbatkina, A.A. Zaitsev, D.A. Sidorenko. Evolution of the microstructure of Cu–Fe–Co–Ni powder mixtures upon mechanical alloying, Powder Technology 276 (2015) 166–174
30. You, J.L. Carbon nanotube grinding wheel for nano machining of engineering and biomedical materials 2009, MSc Thesis , Hong Kong University of Science and Technology
31. W.C. Oliver, G.M. Pharr. Improved technique for determining hardness and elastic modulus using load and displacement sensing indentation experiments // Journal of Materials Research. 1992. – Vol. 7. – Iss. 6. – P. 1564-1580.
32. M.I. Petrzhik, E.A. Levashov. Modern Methods for Investigating Functional Surfaces of Advanced Materials by Mechanical Contact Testing, Crystallography Reports, 2007, Vol. 52, No. 6, pp. 966–974.
33. L. Mishnaevsky Jr., G.M. Dai, Hybrid carbon/glass fiber composites: Micromechanical analysis of structure-damage resistance relationship, Computational Materials Science, Vol. 81, 2014, pp. 630-640
34. Halpin JC, Kardos JL. The Halpin-Tsai equations: a review. Polym Eng Sci 1976; 16: 344- 52.
35. Nielsen, L. E., Generalized equation for the elastic moduli of composite materials. J. Appl. Phys., 1970, 41, 4626–2627
36. Patent Application of Russian Federation № 2015118439 of 18.05.2015, “Composite for Producing the Cutting Tools for Steel and Cast Iron”, authors: Levashov E.A., Loginov P.A., et.al.

Table 1. Phase composition of hot-pressed binder N

Phase	Structural type	Content, % wt	Lattice parameters, Å
Cu-Ni	cF4/1	70	A= 3.580
Fe-Co	cI2/1	30	A= 2.853

Table 2. Phase composition of [Cu-Fe-Co-Ni]-hBN powder following mixing in the PBM

Phase	Str.type	Weight fraction, %	Lattice parameters, Å
α-Fe	cI2/1	48	A=2.858
Ni	cF4/1	20	A=3.523
Cu	cF4/1	32	A=3.615

Table 3. Mechanical properties of hot-pressed Cu-Fe-Co-Ni and [Cu-Fe-Co-Ni]-hBN binders

Composition (wt.%)	H, %	HRB	σ_{bend}, MPa
N	2.4	95	1080±30
N “0”	3.5	95	1100±20
N–0.01%hBN	3.1	102	1160±30
N–0.1%hBN	3.0	102	1260±10
N–0.5%hBN	3.6	100	1140±30
N–1%hBN	4.0	98	1040±30

Table 4. Mechanical properties of hot-pressed N and N – 0.1 % hBN binders

Structural component	N		N-hBN	
	H, GPa	E, GPa	H, GPa	E, GPa
Cu-Ni phase	2.4±0.1	169±12	2.9±0.06	176±15
Fe-Co phase	3.4±0.1	174±10	3.6±0.1	194±13

Table 5. Tensile test results for the original and modified binders

Composition	Rm, MPa	δ, %
N “0”	560	0.4
N – 0.1 % hBN	680	0.6

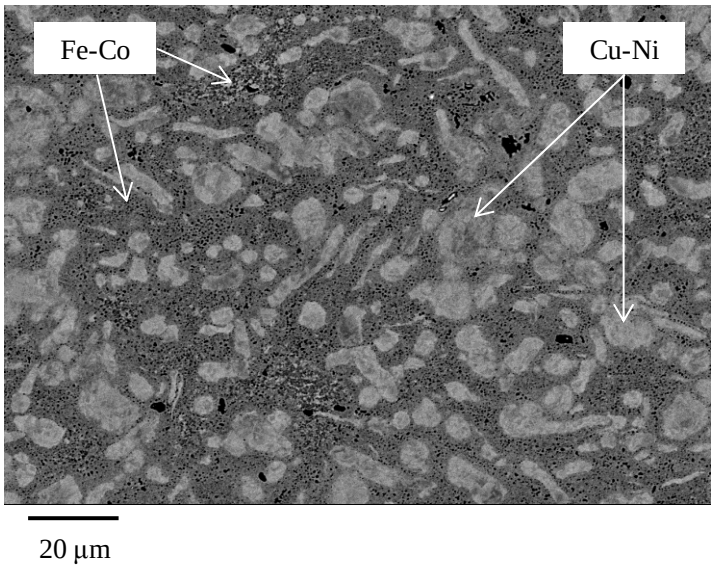

Figure 1. Microstructures of hot-pressed binder N examined by electron microscopy by backscattered electron mode.

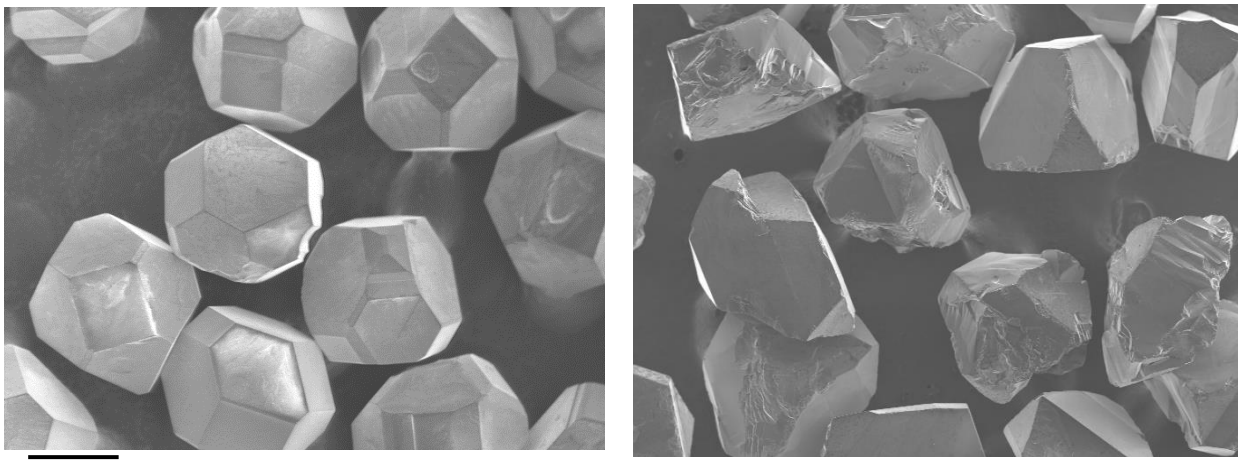

a B

Figure 2. SHM powders used to manufacture cutting tools: a – SDB1100 diamonds, b – ABN 605 cBN.

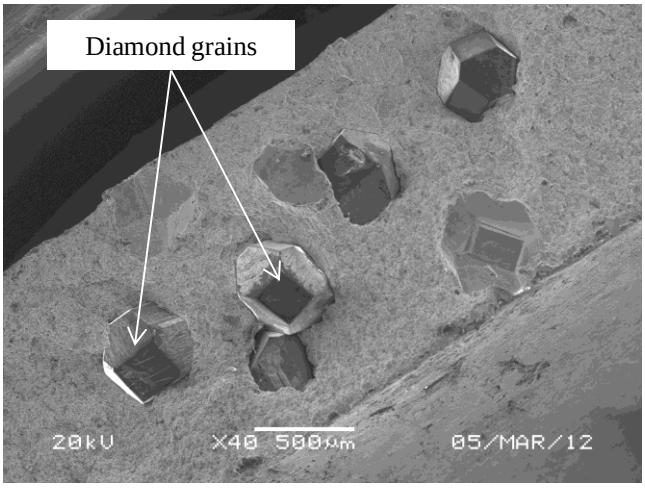

Figure 3. Working layer of a segment with binder N and diamond grains.

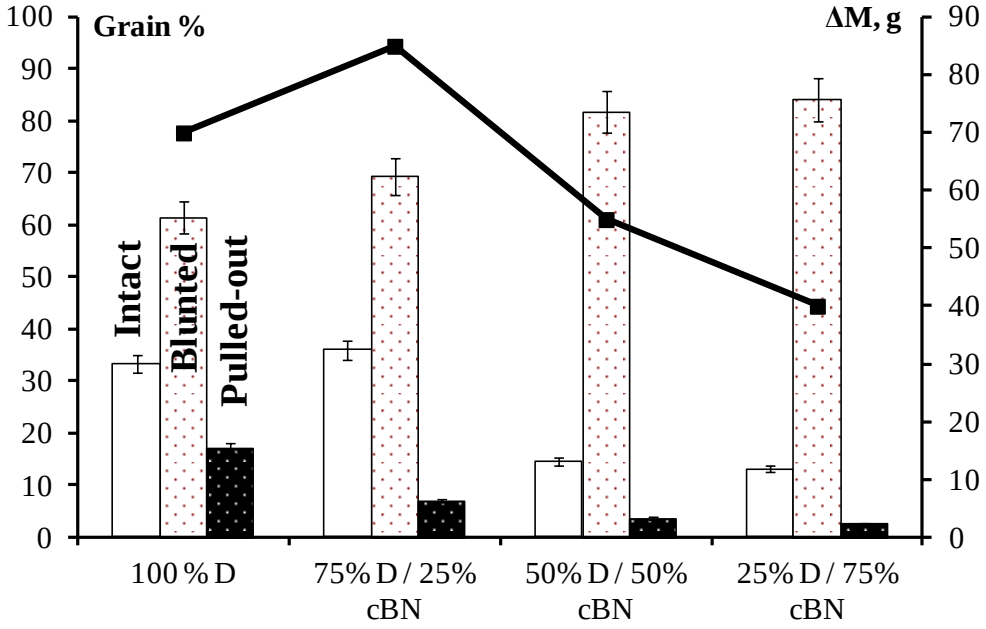

Figure 4. Performance of beads containing diamond and cBN at various ratios and

condition of SHM grains after testing.

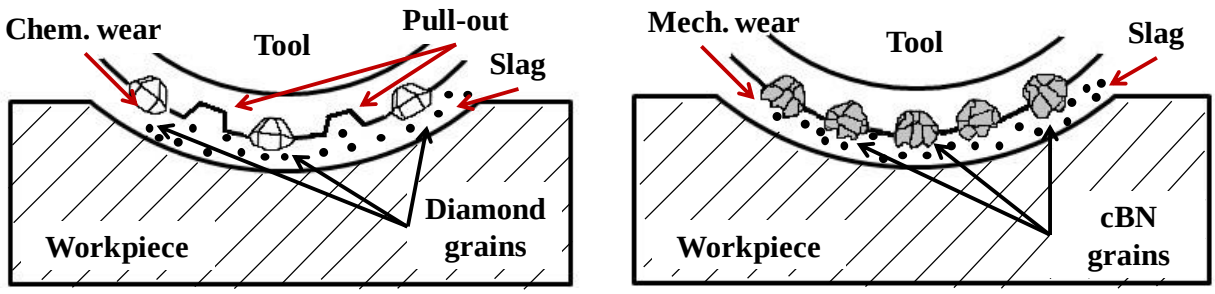

A b

Figure 5. Schemes for cutting steels and cast irons with a tool containing diamond (a) or cBN in the working layer (b)

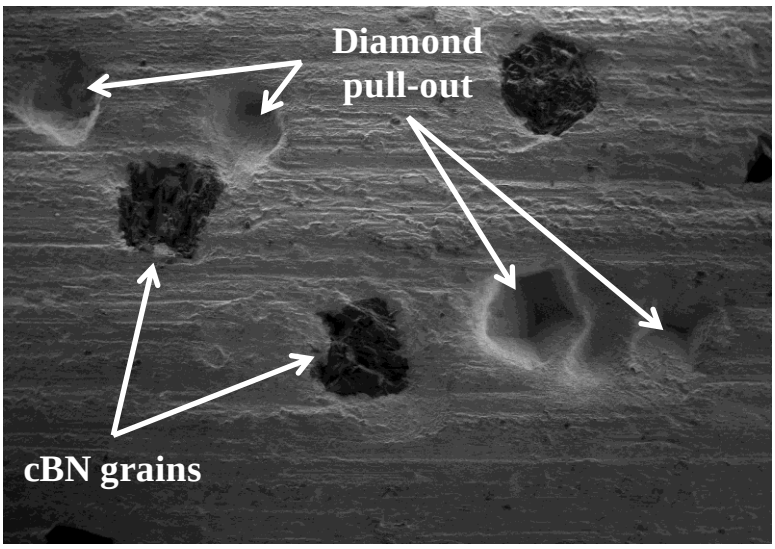

Figure 6. Surface of a bead with a 75/25 diamond to cBN ratio after steel cutting tests.

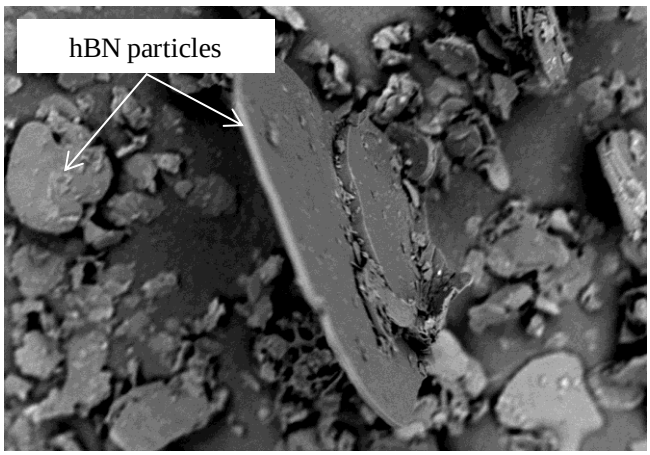

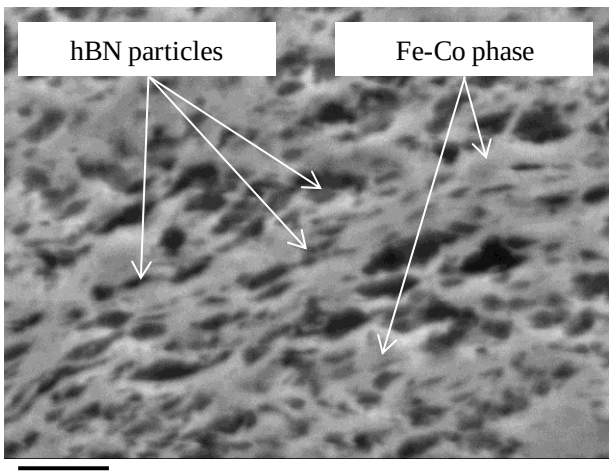

A b

Figure 7. hBN particles before (a) and after mixing with binder components in the PBM (b)

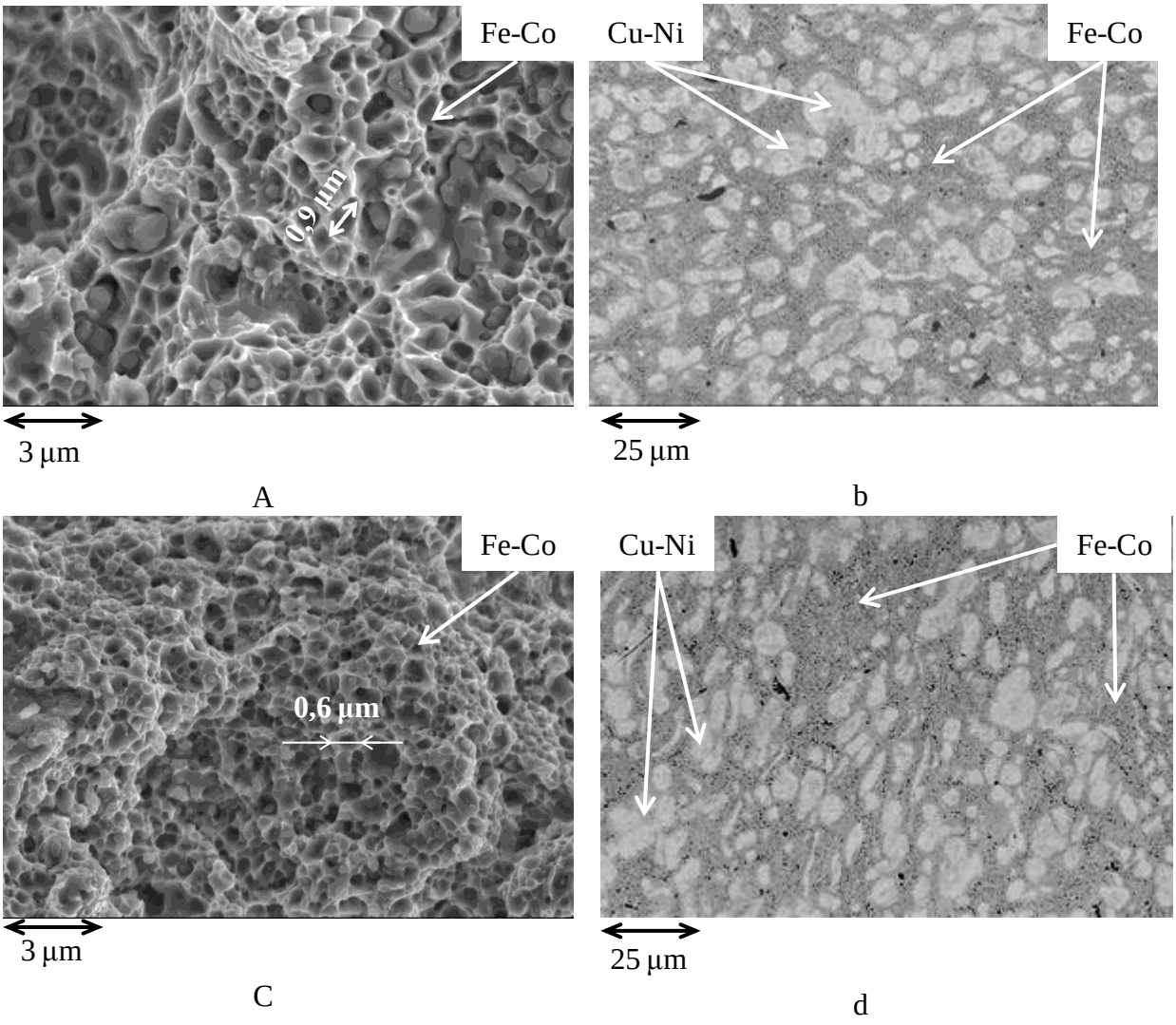

Figure 8. Microstructures of fracture surfaces (a, c) and cross-sections (b, d) of the hot-pressed N (a, b) and N – 0.1 % hBN (c, d) binders

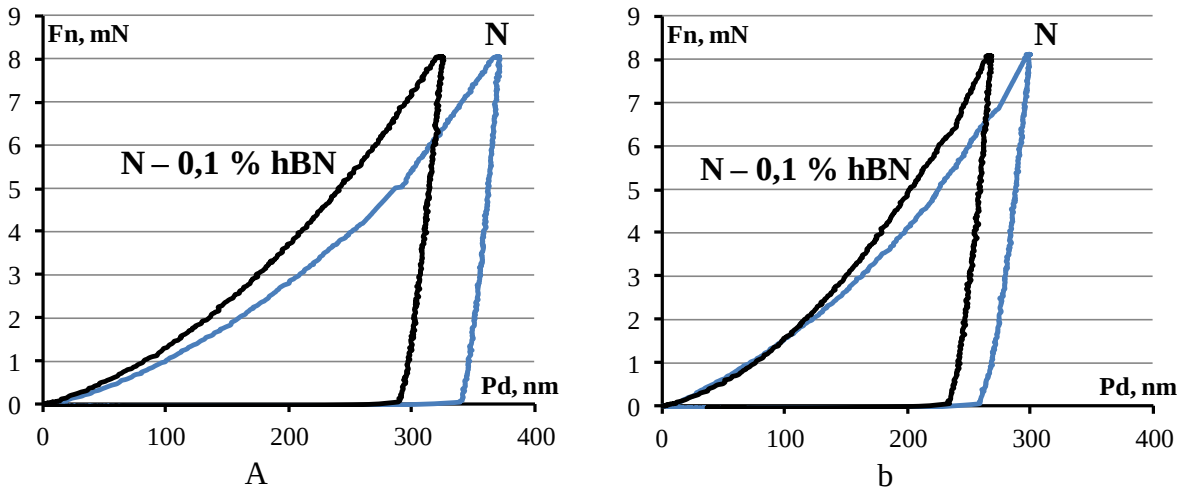

Figure 9. Load curves for the Cu-Ni (a) and Fe-Co (b) phases of N and N – 0.1 % hBN binders

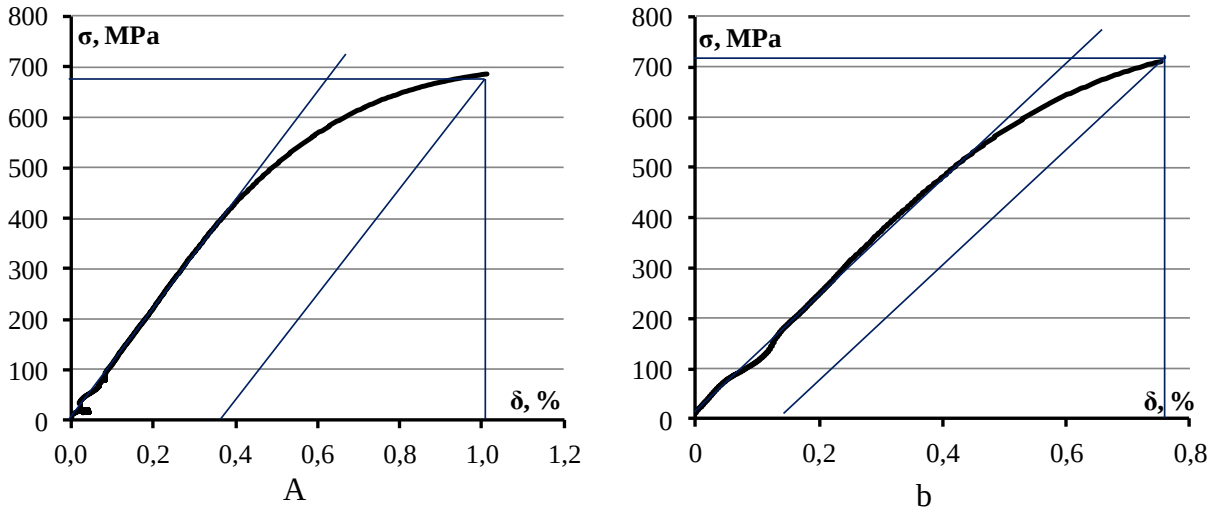

Figure 10. Tensile stress–strain curves recorded for the N and N – 0.1 % hBN binders

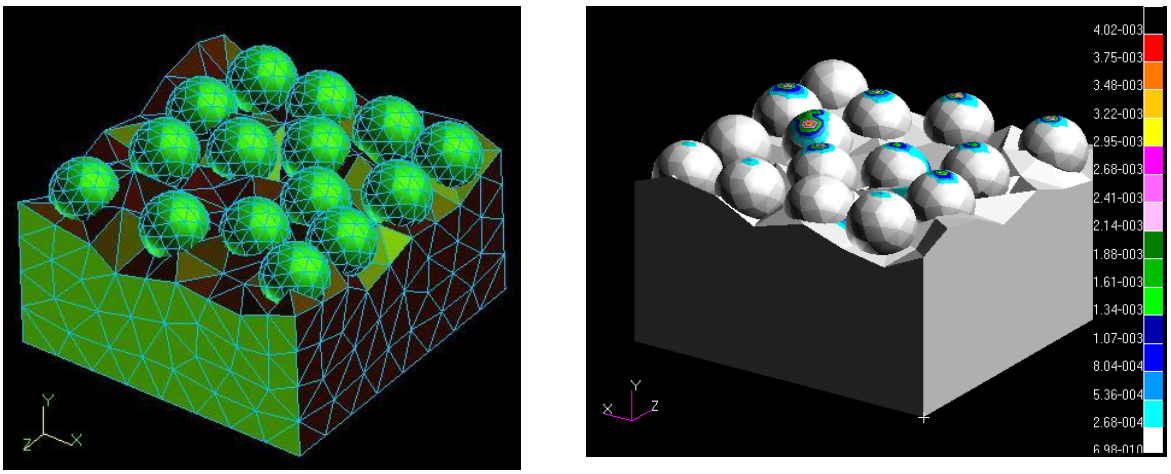

Figure 11. Unit cell finite element model of working surface of grinding wheel [77]

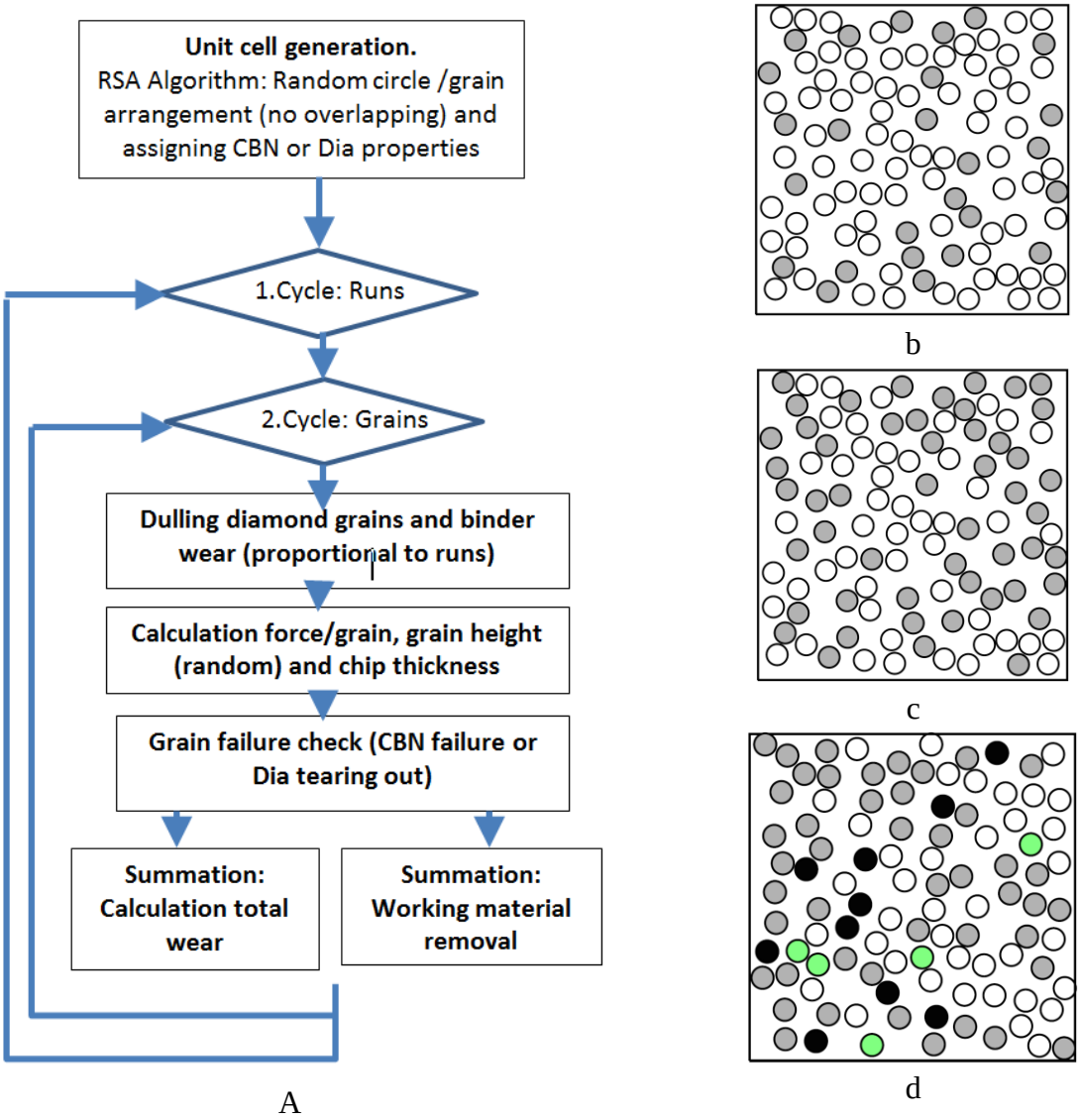

Figure 12. Schema of simulation code (a) and generated unit cells: 20% grains (b), 34& grains (c) and unit cell with failed grains (d)

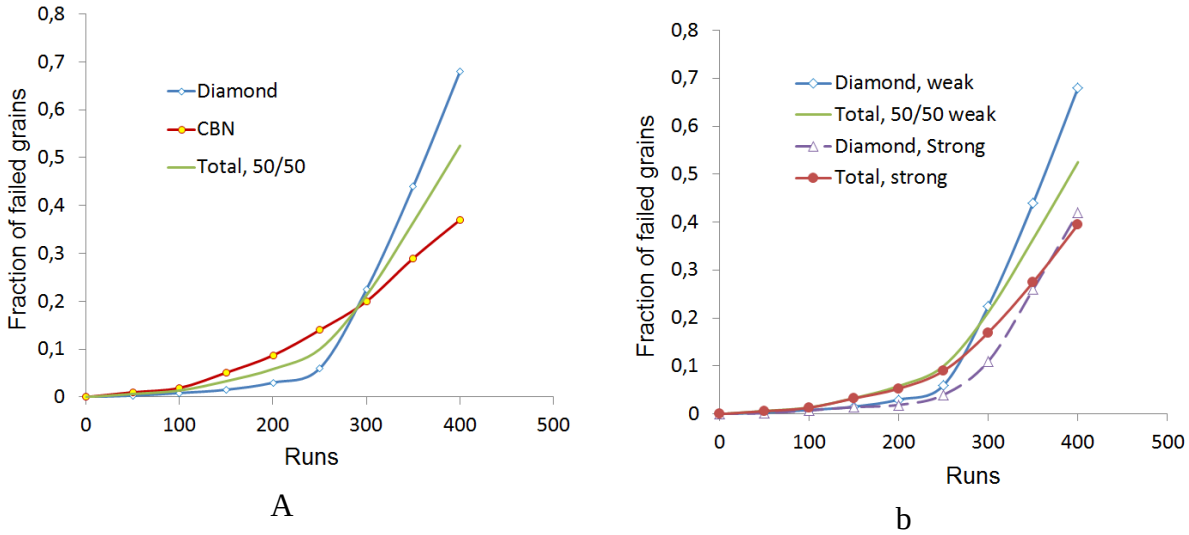

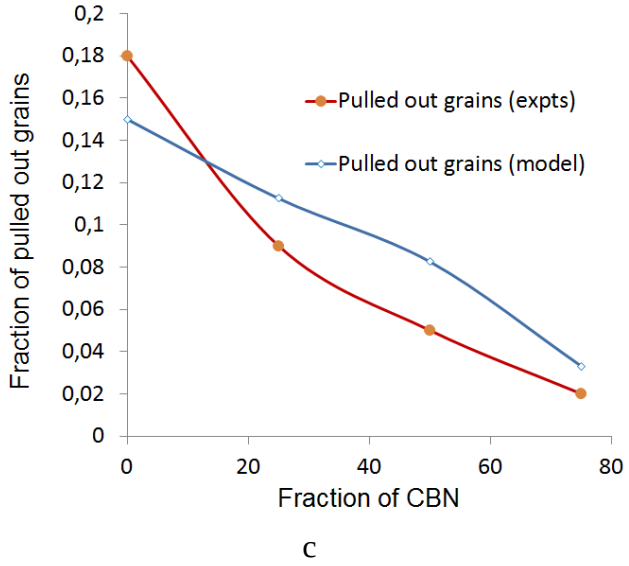

c

Figure 13. Results of grain failure simulations: (a) Diamond, CBN and total grain failure (diamond pulling out, CBN cracking), (b) Comparison for weaker and stronger binders, and (c) Comparison of amount of grains pulled out (experiments and modelling).

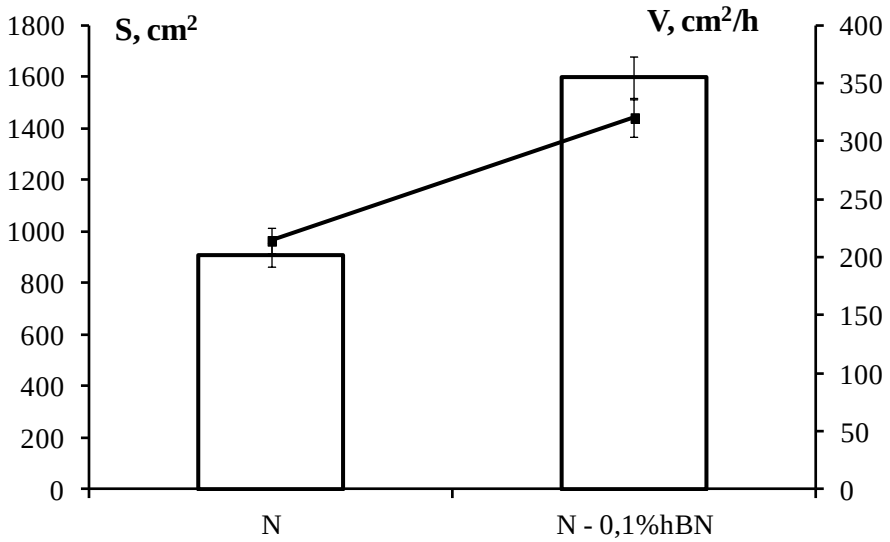

Figure 14. Results of testing segmental cut-off wheels to cut GG20 cast iron.